



Fluorescence quenching detection of peanut agglutinin based on photoluminescent silole-core carbosilane dendrimer peripherally functionalized with lactose

Ken Hatano*, Hitoshi Saeki, Hiroo Yokota, Hiroaki Aizawa, Tetsuo Koyama, Koji Matsuoka, Daiyo Terunuma

Division of Material Science, Graduate School of Science and Technology, Saitama University, 255 Shimo-Ohkubo, Sakura-ku, Saitama 338-8570, Japan

ARTICLE INFO

Article history:

Received 10 June 2009

Revised 17 July 2009

Accepted 31 July 2009

Available online 6 August 2009

Keywords:

Aggregation-induced emission

Biosensor

Carbohydrate

Fluorescence quenching

Glycocluster

Lectin

Silole

ABSTRACT

A glycocluster peripherally functionalized with a lactose (Lac: Gal β 1 \rightarrow 4Glc β 1-) derivative possessing a silole moiety as a luminophore was synthesized. The photoluminescence spectrum of the glycocluster showed extremely strong emission at 474 nm and the absolute quantum yield was estimated to be 92% in distilled water. The emission intensity was decreased by increasing the amount of *peanut agglutinin* (PNA), a lactose-binding lectin, and plots of the relative fluorescence intensity revealed a decline of 95% in emission intensity. Fluorescence quenching of the glycocluster upon mixing with PNA could be easily observed by the naked eye under UV irradiation, whereas no distinct change in fluorescence properties of the glycocluster was observed when *wheat germ agglutinin* (WGA) was employed.

© 2009 Elsevier Ltd. All rights reserved.

Recent advances in glycoscience have revealed that glycoconjugates, such as glycoprotein and glycolipid, generally located on the cell surface play a critical role in the process of cell adhesion with proteins of pathogens.¹ It is known that the early stage of cell adhesion involves carbohydrate-mediated specific recognition of pathogens. Lee et al. discovered that the clustering of carbohydrates leads to the enhancement of individual interactions between carbohydrates and proteins.² A combination of the specific recognition and the carbohydrate cluster effect has been applied for the molecular design of artificial inhibitors and neutralizing agents of pathogens, such as toxins, bacteria, and viruses, and several forms of glycoclusters have been developed so far.³ We have reported the syntheses and biological activities of some glycoclusters in carbosilane dendrimers employed as carbohydrate scaffolds.⁴

On the other hand, glycoclusters possessing luminophores have recently attracted much attention in both clinical and chemical biology fields from the viewpoint of a fluorescent marker that adheres to the target analyte.⁵ However, there have been few reports on the application of luminescent glycoclusters for a biosensor whose emission can be enhanced/quenched or blue/red-shifted in the presence of the target analyte.⁶ We have recently reported the synthesis of not only the first glycocluster possessing siloles (silacyclopentadienes) but also the first hydrophilic silole deriva-

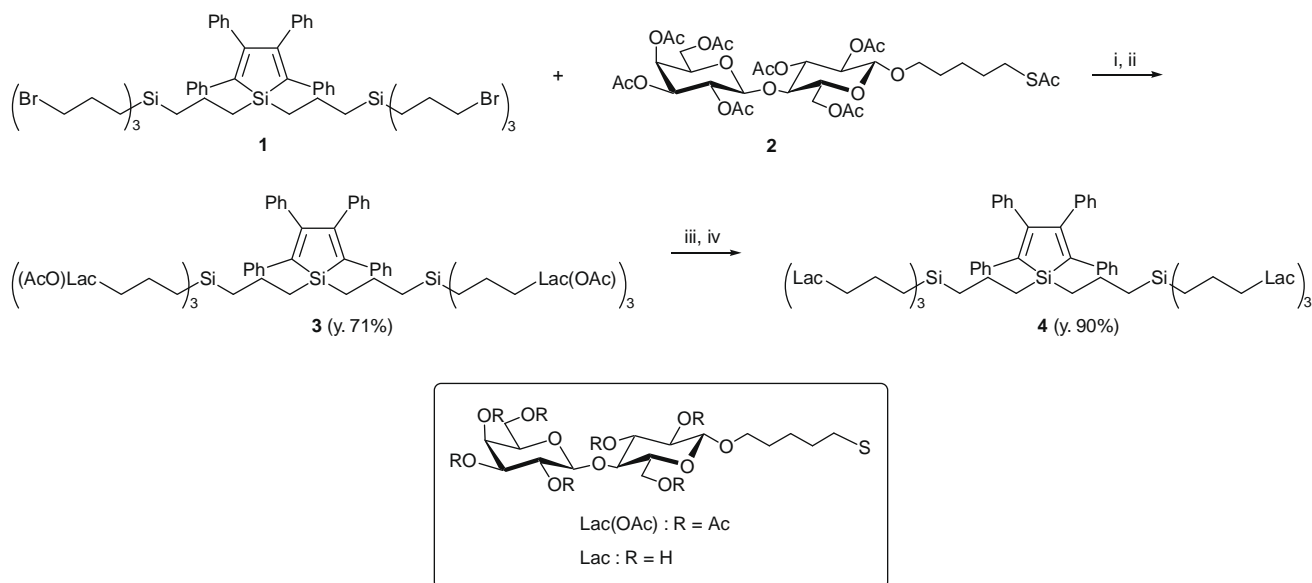
tive, and we have shown that the emission intensity was enhanced by aggregate formation of the silole moiety.⁷ This unique photoluminescence property motivated us to explore the usefulness of the silole-glycocluster as a biosensor of pathogens. In this letter, we present a convenient fluorescence quenching sensor for lectin as an alternate analyte instead of pathogens based upon the aggregation-induced enhanced emission (AIE) feature of silole derivatives.

A glycocluster peripherally functionalized with lactose possessing a silole moiety was prepared according to the same route as that described in our previous report (Scheme 1).⁷ Coupling reaction between a silole-core dendrimer **1** and a peracetylated lactose derivative **2** was achieved by nucleophilic substitution of the terminal bromide on the dendrimer **1** with a thiolate anion generated from **2** by treatment with sodium methoxide in methanol. The silole-core glycodendrimer **3** fully substituted by lactose was obtained in 71% yield after re-acetylation followed by recycling GPC purification.⁸ De-O-acetylation of the glycodendrimer **3** by a combination of Zemplén's condition and saponification afforded the related dendrimer **4**, combining silole-luminophore and lactose moieties having PNA recognition ability, in 90% yield.⁹

A photoluminescence (PL) spectrum of **4** measured in distilled water showed an emission band at around 474 nm from the silole moiety and the absolute quantum yield (Φ_{FL}) was estimated to be 92% in water.¹⁰ Silole luminophore must have some molecular vibrational modes when it is molecularly dissolved in a solvent, and rotation of the phenyl groups linked to the silole nucleus

* Corresponding author. Tel./fax: +81 48 858 3535.

E-mail address: khatano@fms.saitama-u.ac.jp (K. Hatano).



Scheme 1. Reagents and conditions: (i) 28% NaOMe, MeOH, DMF, rt, on; (ii) Ac₂O, pyridine, rt, on; (iii) 28% NaOMe, MeOH, rt, 1 h; (iv) 0.1 M NaOH, rt, on.

may occur mainly in the vibrational modes. Since a considerable part of photo-excited energy would be spent on the phenyl-rotation, low quantum yield and low emission intensity were eventually observed in the solvent. In an aggregational state, however, the phenyl-rotation could be efficiently inhibited by intermolecular repulsion of the phenyl substituents, ultimately resulting in high quantum yield and high emission intensity. The intramolecular restriction of phenyl-rotation may be the main cause for the AIE phenomenon in the case of a π -system peripherally functionalized with phenyl substituents such as silole. Dynamic light scattering (DLS) measurement strongly suggested the formation of monodispersed aggregates of globotriaose analogue of **4** in distilled water (9.0–18.1 nm, 1 mg/100 mL).¹¹ Thus, the extremely high luminescent efficiency of **4** observed in distilled water is attributable to aggregation formation by amphiphilic silole dendrimer **4** in water; the hydrophobic silole groups are oriented within the aggregate and the hydrophilic lactose moieties are exposed to surrounding water.

The PL spectrum of **4** measured in aqueous buffer solution [0.6 μM in HEPES buffer (5 mM, pH 7.4), 3.0 mL] also showed strong emission at 474 nm. Upon addition of PNA solution (20 μM in HEPES buffer), the emission of **4** became faint light. The PL spectra of **4** were obtained with successive addition of aliquots of PNA solution (Fig. 1), and the relative fluorescence intensity $[(I-I_0)/I_0]$, where I_0 and I are emission intensities of **4** in the absence and presence of PNA, respectively, versus PNA concentrations are plotted in Figure 2. The emission intensity decreased progressively with an increase in the amount of PNA and there was a decline of 95% in emission intensity with addition of 50 μL of the PNA solution; however, emission maximums were constantly detected at around 474 nm in all experiments. Fluorescence quenching of **4** upon mixing with PNA can be easily observed by the naked eye under UV irradiation as shown in Figure 3. Analogous treatments of **4** with WGA, a GlcNAc/Neu5Ac-binding lectin, and with a blank solution (buffer solution without lectin) were carried out for comparison. No remarkable fluorescence quenching was detected in both the PL spectra (Fig. 4); additions of 80 μL of each solution led to a decline of only 2% in emission intensity due to the diluting effect. Therefore, the variations of emission intensity from **4** were essentially inert, unlike the case of PNA, clearly indicating that silole dendrimer **4** specifically recognizes PNA. A

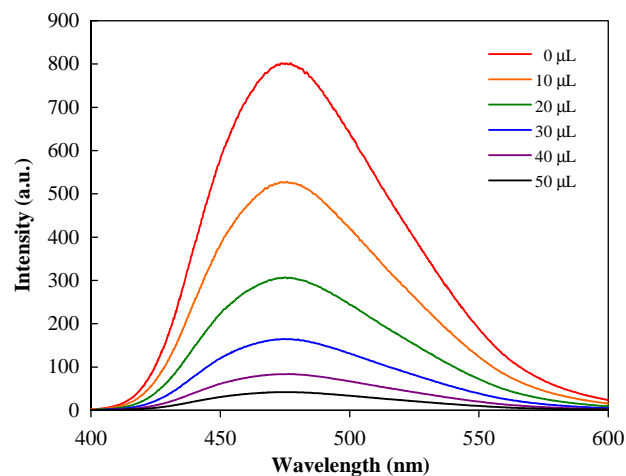


Figure 1. PL spectra of silole-core dendrimers **4** in the presence of different amounts of PNA (from 0 to 50 μL). Concentration of **4**: 0.6 μM in HEPES buffer (5 mM, pH 7.4). Concentration of PNA: 20 μM in HEPES buffer (5 mM, pH 7.4). Excitation: 360 nm.

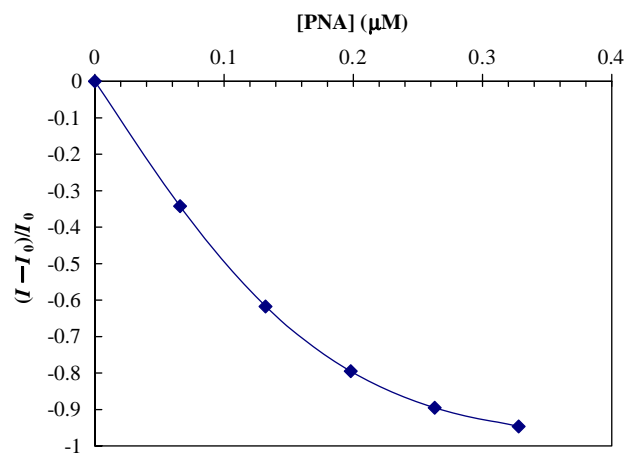


Figure 2. Plots of relative fluorescence intensity $[(I-I_0)/I_0]$ of solution of **4** at 474 nm versus concentration of PNA.

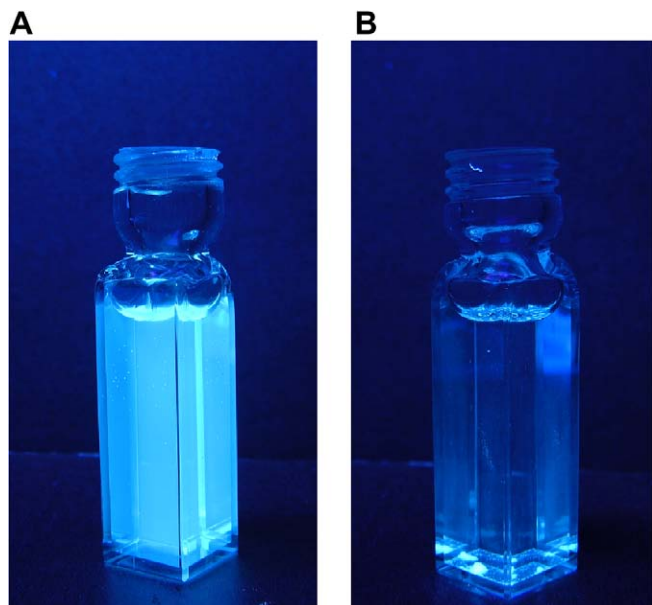


Figure 3. Pictures of photoluminescence of the HEPES buffer solution of **4** in the (A) absence and (B) presence of PNA. Excitation: 360 nm.

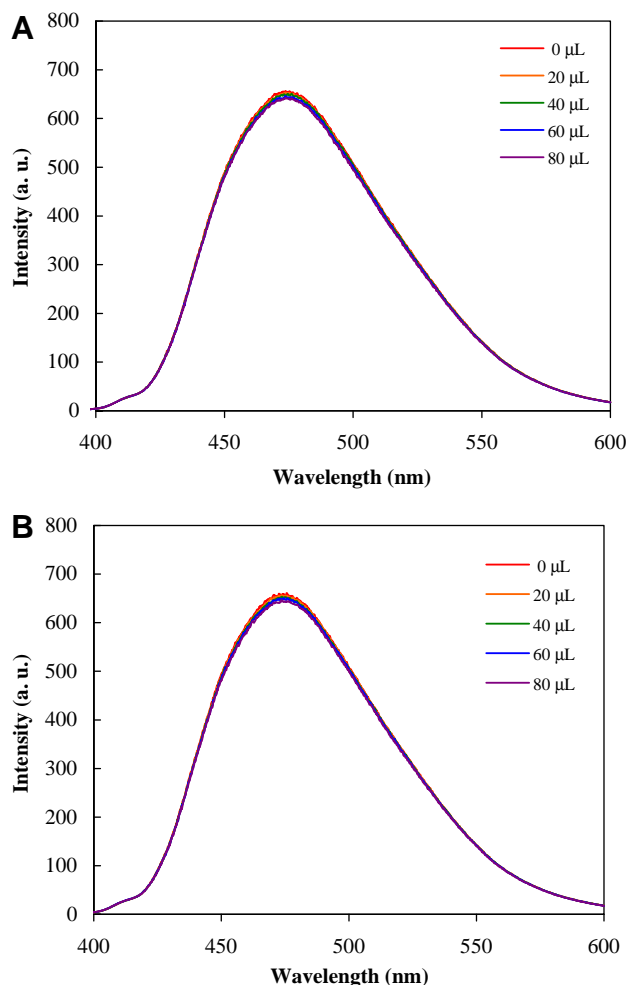


Figure 4. PL spectra of silole-core dendrimers **4**. (A): Presence of different amounts of WGA (from 0 to 80 μ L). Concentration of **4**: 0.6 μ M in HEPES buffer (5 mM, pH 7.4). Concentration of WGA: 40 μ M in HEPES buffer (5 mM, pH 7.4). Excitation: 360 nm. (B): Addition of different amounts of blank solution (from 0 to 80 μ L). Excitation: 360 nm.

plausible mechanism for the fluorescence quenching of **4** upon mixing with PNA is agglomerate dispersion of **4** formed in the absence of the lectin due to carbohydrate–lectin specific recognition, that is, PNA addition converts a highly emissive ‘AIE active’ situation of silole **4** into a non-emissive ‘AIE inactive’ situation. Silole-core dendrimers peripherally functionalized with carbohydrates such as **4** are potentially useful for detection of a target lectin by means of the high affinity and specificity of the glycocluster and the AIE effect of the silole derivative. Further investigations of silole-core dendrimers functionalized with bioactive oligosaccharides and their applications to detection of pathogens as a novel biosensor are currently in progress.

Acknowledgments

This work was supported by a Grant-in-Aid for Scientific Research (C) (No. 21550152) from the Japan Society for the Promotion of Science. We thank Professor K. Tamao, Dr. T. Matsuo and Dr. T. Fukawa [The Institute of Physical and Chemical Research (RIKEN)] for measurements of absolute quantum yield of the silole dendrimers.

Supplementary data

Supplementary data (analytical data for new compounds) associated with this article can be found, in the online version, at doi:10.1016/j.tetlet.2009.07.153.

References and notes

- (a) Lis, H.; Sharon, N. *Chem. Rev.* **1998**, *98*, 637–674; (b) Mammen, M.; Choi, S. K.; Whitesides, G. M. *Angew. Chem., Int. Ed.* **1998**, *37*, 2755–2794; (c) Jelinek, R.; Kolusheva, S. *Chem. Rev.* **2004**, *104*, 5987–6015.
- (a) Lee, Y. C.; Townsend, M. R.; Hardy, M. R.; Lönnngren, J.; Arnarp, J.; Haraldsson, M.; Lönn, H. J. *Biol. Chem.* **1983**, *258*, 199–202; (b) Lee, Y. C. *FASEB J.* **1992**, *6*, 3193–3200.
- See following reviews and references cited therein: (a) Lundquist, J.-J.; Toone, E. J. *Chem. Rev.* **2002**, *102*, 555–578; (b) Chabre, Y. M.; Roy, R. *Curr. Top. Med. Chem.* **2008**, *8*, 1237–1285; (c) Schengrund, C.-L. *Biochem. Pharm.* **2003**, *65*, 699–707.
- (a) Matsuoka, K.; Terabatake, M.; Esumi, Y.; Terunuma, D.; Kuzuhara, H. *Tetrahedron Lett.* **1999**, *40*, 7839–7842; (b) Matsuoka, K.; Kurosawa, H.; Esumi, Y.; Terunuma, D.; Kuzuhara, H. *Carbohydr. Res.* **2000**, *329*, 765–772; (c) Matsuoka, K.; Oka, H.; Koyama, T.; Esumi, Y.; Terunuma, D. *Tetrahedron Lett.* **2001**, *42*, 3327–3330; (d) Matsuoka, K.; Ohtawa, T.; Hinou, H.; Koyama, T.; Esumi, Y.; Nishimura, S.-I.; Hatano, K.; Terunuma, D. *Tetrahedron Lett.* **2003**, *44*, 3617–3620; (e) Mori, T.; Hatano, K.; Matsuoka, K.; Esumi, Y.; Toone, E. J.; Terunuma, D. *Tetrahedron* **2005**, *61*, 2751–2760; (f) Yamada, A.; Hatano, K.; Koyama, T.; Matsuoka, K.; Esumi, Y.; Terunuma, D. *Carbohydr. Res.* **2006**, *341*, 467–473; (g) Yamada, A.; Hatano, K.; Koyama, T.; Matsuoka, K.; Takahashi, N.; Hidari, K. I. P. J.; Suzuki, T.; Suzuki, Y.; Terunuma, D. *Bioorg. Med. Chem.* **2007**, *15*, 1606–1614; (h) Sakamoto, J.-I.; Koyama, T.; Miyamoto, D.; Yingsakmongkon, S.; Hidari, K. I. P. J.; Jampangern, W.; Suzuki, T.; Suzuki, Y.; Esumi, Y.; Hatano, K.; Terunuma, D.; Matsuoka, K. *Bioorg. Med. Chem. Lett.* **2007**, *17*, 717–721.
- (a) Hatano, K.; Yamazaki, T.; Yoshino, K.; Ohya, N.; Koyama, T.; Matsuoka, K.; Terunuma, D. *Tetrahedron Lett.* **2008**, *49*, 5593–5596; (b) Guo, Z.; Lei, A.; Zhang, Y.; Xu, Q.; Xue, X.; Zhang, F.; Liang, X. *Chem. Commun.* **2007**, 2491–2493; (c) Peng, J.; Wang, K.; Tan, W.; He, X.; He, C.; Wu, P.; Liu, F. *Talanta* **2007**, *71*, 833–840.
- Nanoparticles scaffolds: (a) Huang, C.-C.; Chen, C.-T.; Shiang, Y.-C.; Lin, Z.-H.; Chang, H.-T. *Anal. Chem.* **2009**, *81*, 875–882; (b) Otsuk, H.; Akiyama, Y.; Nagasaki, Y.; Kataoka, K. *J. Am. Chem. Soc.* **2001**, *123*, 8826–8830; (c) Uzawa, H.; Ohga, K.; Shinozaki, Y.; Ohsawa, I.; Nagatsuka, T.; Seto, Y.; Nishida, Y. *Biosens. Bioelectron.* **2008**, *24*, 923–927; Polymers scaffolds: (d) Kikkeri, R.; Lepenies, B.; Adibekian, A.; Laurino, P.; Seeberger, P. H. *J. Am. Chem. Soc.* **2009**, *131*, 2110–2112; (e) Baek, M. G.; Stevens, R.; Charych, D. H. *Bioconjugate Chem.* **2000**, *11*, 777–788; (f) Xue, C.; Kuo, F. T.; Liu, H. *Macromolecules* **2007**, *40*, 6863–6870.
- Hatano, K.; Aizawa, H.; Yokota, H.; Yamada, A.; Esumi, Y.; Koshino, H.; Koyama, T.; Matsuoka, K.; Terunuma, D. *Tetrahedron Lett.* **2007**, *48*, 4365–4368.
- Compound 3**: $[\alpha]_D^{25} -8.7$ (c 1.0, CHCl₃). ¹H NMR: (CDCl₃, 400 MHz) δ 6.73–7.12 (m, 20H, aromatic), 5.34 (d, 6H, *J* = 2.8 Hz, H-4'), 5.18 (t, 6H, *J* = 9.6 Hz, H-3), 5.10 (t, 6H, *J* = 8.0 Hz, H-2'), 4.95 (dd, 6H, *J*_{3',4'} = 2.8 Hz, *J*_{2,3'} = 10.4 Hz, H-3'), 4.87 (t, 6H, *J* = 8.4 Hz, H-2), 4.43–4.49 (m, 18H, H-1, H-1', H-6b), 4.04–4.15 (m, 18H, H-6a, H-6'ab), 3.87 (t, 6H, *J* = 6.4 Hz, H-5'), 3.76–3.85 (m, 12H, H-4, OCH₂b), 3.56–3.60 (m, 6H, H-5), 3.40–3.46 (m, 6H, OCH₂a), 2.42 (br s, 24H, SCH₂), 1.96–2.15 (m, 126H, OAc), 1.51–1.61 (m, 24H, OCH₂CH₂CH₂), 1.37–1.49 (m, 28H, SCH₂CH₂, SiCH₂CH₂), 1.05–1.07 (m, 4H, SiCH₂CH₂CH₂SiCH₂), 0.47–0.56

- (m, 16H, $\text{SCH}_2\text{CH}_2\text{CH}_2\text{SiCH}_2$). ^{13}C NMR (CDCl_3 , 100 MHz) δ 170.17, 170.14, 169.96, 169.86, 169.62, 169.39, 168.90, 154.96, 140.37, 139.98, 138.66, 129.75, 128.71, 127.81, 127.28, 126.05, 125.34, 100.86, 100.37, 76.11, 72.66, 72.42, 71.51, 70.80, 70.46, 69.72, 68.94, 66.45, 61.87, 60.63, 35.88, 31.90, 29.18, 28.89, 24.95, 24.05, 20.69, 20.63, 20.54, 20.44, 20.32, 18.24, 16.68, 16.41, 11.81. IR (KBr) 2938 (w, sh), 1781 (s, sh), 1437 (w, sh), 1369 (m, sh), 1233 (s, sh), 1171 (w, sh), 1132 (w, sh), 1051 (m, sh) cm^{-1} . UV-vis (CHCl_3) λ_{max} 361 nm ($\epsilon = 8300$). MALD-TOF calcd for $\text{C}_{238}\text{H}_{338}\text{O}_{108}\text{S}_6\text{Si}_3\text{Na}$ $[\text{M}+\text{Na}]^+$ 5225.855; found 5226.436.
9. **Compound 4**: $[\eta]_{\text{D}}^{37}$ 45.0 (c 1.0, H_2O). ^1H NMR (D_2O , 400 MHz) δ 6.41–7.15 (br m, 20 H, aromatic), 4.29–4.51 (br m, 12H, H-1, H-1'), 3.21–4.10 (br m, 78H, CH_2O , H-2, H-3, H-4, H-5, H-6ab, H-2', H-3', H-4', H-5', H-6'ab), 2.22–2.65 (br s, 24H, CH_2SCH_2), 1.18–1.84 (m, 52H, $\text{OCH}_2\text{CH}_2\text{CH}_2\text{CH}_2\text{SCH}_2\text{CH}_2\text{CH}_2\text{SiCH}_2\text{CH}_2$), 0.85–1.13 (br s, 4H, $\text{SiCH}_2\text{CH}_2\text{CH}_2\text{SiCH}_2$), 0.20–0.75 (br, 16H, SiCH_2). ^{13}C NMR (D_2O , 100 MHz) δ 140.19, 137.18, 125.50–129.69 (br m), 102.77, 102.18, 78.29, 75.07, 74.44, 74.30, 73.01, 72.56, 72.38, 70.70, 70.35, 69.92, 69.69, 68.29, 67.80, 60.77, 60.09, 35.44, 32.12, 31.51, 29.23, 28.75, 28.32, 24.81, 23.86, 18.32, 16.91, 11.46. IR (KBr) 3383 (s, br), 2922 (m, sh), 1643 (w, br), 1416 (w, br), 1074 (s, br) cm^{-1} . UV-vis (water) λ_{max} 360 nm ($\epsilon = 6700$). MALD-TOF calcd for $\text{C}_{154}\text{H}_{254}\text{O}_{66}\text{S}_6\text{Si}_3\text{Na}$ $[\text{M}+\text{Na}]^+$ 3460.409; found 3458.414.
10. The quantum yield was determined by means of the absolute PL quantum measurement system C9920-03 (Hamamatsu Photonics K. K.). The Φ_{FL} is the second highest efficiency in silole derivatives, following 1,2-bis(1-methyl-2,3,4,5-tetraphenylsilacyclopentadienyl)ethane reported by Murata et al. Murata, H.; Kafafi, Z. H.; Uchida, M. *Appl. Phys. Lett.* **2002**, *80*, 189–191.
11. More details, including DLS measurement in distilled water, will be published elsewhere.